

Thermal non-equilibrium modeling of heat transfer through vertical annulus embedded with porous medium

Irfan Anjum Badruddin^{a,*}, Z.A. Zainal^a, P.A. Aswatha Narayana^b, K.N. Seetharamu^c

^a School of Mechanical Engineering, Universiti Sains Malaysia, 14300 Nibong Tebal, Pulau Pinang, Malaysia

^b MS Ramaiah School of Advanced Studies, Gnanagangothri Campus, New BEL Road, Bangalore 560 054, India

^c Sri Bhagawan Mahavir Jain College of Engineering, Jakkasandra Post, Kanakapura Taluk, Bangalore 562 112, India

Received 28 October 2005; received in revised form 2 February 2006

Available online 7 September 2006

Abstract

Present study is undertaken to investigate the steady state heat transfer in a porous medium fixed in a vertical annular cylinder. A two-temperature, thermal non-equilibrium model is used to analyse the heat transfer behavior in the porous medium. The Darcy model of flow is employed. The inner surface of the vertical annulus is maintained at constant wall temperature and the outer surface remains at ambient temperature. The heat transfer is assumed to take place by natural convection and radiation. The equations governing the flow behavior are non-dimensionalised using suitable non-dimensional parameters and then solved using finite element method. Three-node triangular element is used to mesh the domain. The effect of various parameters such as aspect ratio, radius ratio of annulus, modified conductivity ratio, inter-phase heat transfer coefficient, radiation parameter and Rayleigh number on the heat transfer behavior is discussed.

© 2006 Elsevier Ltd. All rights reserved.

Keywords: Vertical annulus; Porous medium; Natural convection; Radiation; Thermal non-equilibrium model; FEM

1. Introduction

It is well known fact that the understanding of heat transfer in the porous medium is increasing rapidly. This can be attributed to the intense interest of many researchers to estimate the heat and fluid flow behavior of porous medium enclosed/embedded by various geometries. The deep interest in the porous medium is easily understandable since porous medium is used in vast applications, which covers many engineering disciplines. For instance, applications of the porous media includes, thermal insulations of buildings, heat exchangers, solar energy collectors, geophysical applications, solidification of alloys, nuclear waste disposal, drying processes, chemical reactors, petroleum resources etc. to name but few. More applications and good understanding of the subject is given in the recent books by Nield and Bejan [1], Vafai [2], Pop and Ingham

[3], Ingham and Pop [4]. There are two different approaches of modeling the heat transfer in porous medium namely, thermal equilibrium and thermal non-equilibrium modeling. In case of the thermal equilibrium modeling, the fluid phase and the solid phase of porous medium are assumed to be in thermal equilibrium and thus only one energy equation is required to predict the heat transfer behavior. In case of the thermal non-equilibrium modeling, the fluid and the solid phases are not in thermal equilibrium condition thus fluid and solid have different temperatures. In this case, two energy equations i.e. one for the fluid and another for the solid matrix is considered, which are coupled by convection term between them. Plenty of work has been carried out considering the thermal equilibrium model, whereas the thermal non-equilibrium modeling of the porous medium has not received as much attention as compared to thermal equilibrium model. Yih [5] has studied the effect of radiation on natural convection over a vertical cylinder using thermal equilibrium model. Hossain and Alim [6] have applied thermal equilibrium model to

* Corresponding author. Tel.: +60 4 5995999x6369; fax: +60 4 5941025.
E-mail address: Irfan_magami@Rediffmail.com (I. Anjum Badruddin).

Nomenclature

| | | | |
|--------------------|--|----------------------|------------------------------------|
| Ar | aspect ratio = $\frac{C}{r_o - r_i}$ | u | velocity in r -direction |
| C | cylinder height | w | velocity in z -direction |
| c_p | specific heat | <i>Greek symbols</i> | |
| g | gravitational acceleration | α | thermal diffusivity |
| h | convective heat transfer coefficient | β | coefficient of volume expansion |
| H | inter-phase heat transfer coefficient | β_R | Rosseland extinction coefficient |
| k | thermal conductivity | γ | modified conductivity ratio |
| K | permeability of porous media | ρ | density |
| L_{ref} | reference length | ν | coefficient of kinematic viscosity |
| n | refractive index | ϕ | porosity |
| N | shape function | σ | Stephan Boltzmann constant |
| \overline{Nu} | average Nusselt number | ψ | stream function |
| q_r | radiation flux | $\overline{\psi}$ | non-dimensional stream function |
| q_t | total heat flux | <i>Subscripts</i> | |
| r, z | cylindrical co-ordinates | w | wall |
| \bar{r}, \bar{z} | non-dimensional co-ordinates | ∞ | conditions at outer radius |
| r_i, r_o | inner and outer radius | f | fluid |
| Ra | Rayleigh number | S | solid |
| R_d | radiation parameter | t | total |
| Rr | radius ratio = $\frac{r_o - r_i}{r_i}$ | | |
| T | temperature | | |
| \overline{T} | non-dimensional temperature | | |

investigate the natural convection radiation interaction on boundary layer flow along vertical cylinder. They used two different methods i.e. local non-similarity method and implicit finite difference scheme with Keller box elimination method. Prasad and Kulacki [7] have reported the numerical investigation of natural convection in a vertical annulus filled with saturated porous medium. Prasad [8] also studied the natural convection in vertical porous annulus when the inner wall is maintained at constant heat flux. Their study suggests that the heat transfer rate is higher when the inner surface is maintained at constant heat flux as compared to the case of isothermal wall temperature. Prasad et al. [9] have conducted experimental study as well for the case of natural convection in a vertical annular cylinder filled with saturated porous medium by applying constant heat flux at inner wall and isothermally cooling outer surface. Rajamani et al. [10] have studied the natural convective heat transfer in an annular cylinder by assuming the thermal equilibrium model. There are various applications, which involves thermal non-equilibrium condition between the fluid phase and the solid matrix of the porous media. Recent years have seen an increased use of thermal non-equilibrium modeling. Rees et al. [11] have investigated the forced convection past a heated cylinder in a porous medium by employing the thermal non-equilibrium model and found that the heat transfer coefficient do not vary in the tangential direction of cylinder when the porous medium is in thermal equilibrium condition. However, the heat transfer coefficients varied when the system comes under

non-equilibrium condition. Wong et al. [12] have supplemented the work of Rees et al. [11] for finite Peclet number. Baytas and Pop [13] have studied the free convection in a porous cavity using the thermal non-equilibrium model by employing the cell-centered finite volume scheme. Jiang and Ren [14] have investigated the forced convection heat transfer in a porous media using the thermal non-equilibrium model. They found that the fluid temperature is higher when the viscous dissipation is considered than the case when viscous dissipation is not been considered. Saeid [15] has considered the non-equilibrium model to analyse the mixed convection in a vertical porous layer by using finite volume method and found that, for the mixed convection region, the total average Nusselt number is more for lower Rayleigh number than that for higher Rayleigh number. Saeid [16] also studied the periodic free convection from a vertical plate using thermal non-equilibrium model. Analysis of non-Darcian effects by using two-temperature model in the porous media has been carried out by Marafie and Vafai [17]. They found that the temperature difference between the fluid and the solid phases decreases with increasing Biot number. Cherif and Sifaoui [18,19] and Sghaier et al. [20] have studied the radiation heat transfer in porous media enclosed in a cylindrical and spherical geometry. They have used Runge–Kutta method and finite difference method, respectively to solve the governing equations. Rees and Pop [21] have considered the non-equilibrium model to study the free convection stagnation point flow in a porous medium. Rees and Pop [22] have also

studied the free convection boundary layer flow from a vertical surface in a porous medium.

The present work is aimed to study the heat transfer by convection and radiation in an annular vertical cylinder filled with saturated porous medium, using a two-temperature thermal non-equilibrium model and thus predict the temperature of the fluid and solid matrix. To the best of our knowledge, the study of heat transfer by convection and radiation through vertical annulus filled with saturated porous medium using thermal non-equilibrium model has not been reported so far. Finite element method is employed to solve the governing partial differential equations. Results are presented in terms of isotherms and Nusselt number for various values of the aspect ratio, radius ratio, inter-phase heat transfer coefficient, modified conductivity ratio, radiation parameter and Rayleigh number.

2. Analysis

A vertical annular cylinder with inner radius r_i and outer radius r_o is considered in the present study. The vertical annulus is filled with the saturated porous medium between inner and outer surfaces. The r and z axis points towards the radial and vertical direction of the annulus. The inner surface of the annulus is heated to constant temperature T_w and the outer surface is maintained at constant temperature T_∞ such that $T_w > T_\infty$. The following assumptions are applied:

- (a) The fluid follows Darcy law.
- (b) The convective fluid and the porous medium are not in local thermodynamic equilibrium.
- (c) There is no phase change of the fluid in the medium.
- (d) The properties of the fluid and those of the porous medium are homogeneous and isotropic.
- (e) Fluid properties are constant except the variation of density with temperature.
- (f) The fluid is transparent to radiation.
- (g) The radiative heat flux in the z -direction is negligible in comparison to that in the r -direction.

The governing equations that describe the flow behavior can be written as:

$$\frac{\partial(ru)}{\partial r} + \frac{\partial(rw)}{\partial z} = 0 \tag{1}$$

$$\frac{\partial w}{\partial r} - \frac{\partial u}{\partial z} = \frac{gK\beta}{v} \frac{\partial T}{\partial r} \tag{2}$$

$$(\rho c_p)_f \left(u \frac{\partial T_f}{\partial r} + w \frac{\partial T_f}{\partial z} \right) = \phi k_f \left(\frac{1}{r} \frac{\partial}{\partial r} \left(r \frac{\partial T_f}{\partial r} \right) + \frac{\partial^2 T_f}{\partial z^2} \right) + h(T_s - T_f) \tag{3}$$

$$(1 - \phi)k_s \left(\frac{1}{r} \frac{\partial}{\partial r} \left(r \frac{\partial T_s}{\partial r} \right) + \frac{\partial^2 T_s}{\partial z^2} \right) = h(T_s - T_f) + (1 - \phi) \frac{1}{r} \frac{\partial}{\partial r} (r q_r) \tag{4}$$

Corresponding boundary conditions are:

$$\text{at } r = r_i, \quad T_f = T_s = T_w, \quad u = 0 \tag{5a}$$

$$\text{at } r = r_o, \quad T_f = T_s = T_\infty, \quad u = 0 \tag{5b}$$

where u and w are Darcy's velocities in the r and z directions, respectively.

The continuity equation (1) can be satisfied automatically by introducing the stream function ψ as

$$u = -\frac{1}{r} \frac{\partial \psi}{\partial z} \tag{6}$$

$$w = \frac{1}{r} \frac{\partial \psi}{\partial r} \tag{7}$$

Invoking Rosseland approximation for radiation [23]

$$q_r = -\frac{4n^2\sigma}{3\beta_R} \frac{\partial T^4}{\partial r} \tag{8}$$

The term T^4 in Eq. (8) can be expanded in Taylor series. Expanding T^4 about T_∞ [24] and neglecting higher order terms results as

$$T^4 \approx 4TT_\infty^3 - 3T_\infty^4 \tag{9}$$

The following parameters have been used for non-dimensionalisation of the governing equations:

$$\begin{aligned} \bar{r} &= \frac{r}{L_{\text{ref}}}, \quad \bar{z} = \frac{z}{L_{\text{ref}}}, \quad \bar{\psi} = \frac{\psi}{\alpha\phi L_{\text{ref}}}, \\ \bar{T} &= \frac{(T - T_0)}{(T_w - T_\infty)} \quad \text{where } T_0 = \frac{(T_w + T_\infty)}{2}, \quad R_d = \frac{4\sigma n^2 T_\infty^3}{\beta_R k_s}, \\ Ra &= \frac{g\beta\Delta T K L_{\text{ref}}}{\phi\nu\alpha_f}, \quad H = \frac{hL_{\text{ref}}^2}{\phi k_f}, \quad \gamma = \frac{\phi k_f}{(1 - \phi)k_s} \end{aligned} \tag{10}$$

Substitution of Eqs. (6)–(10) into Eqs. (2)–(4) results into:

$$\frac{\partial^2 \bar{\psi}}{\partial \bar{z}^2} + \bar{r} \frac{\partial}{\partial \bar{r}} \left(\frac{1}{\bar{r}} \frac{\partial \bar{\psi}}{\partial \bar{r}} \right) = \bar{r} Ra \frac{\partial \bar{T}_f}{\partial \bar{r}} \tag{11}$$

$$\frac{1}{\bar{r}} \left[\frac{\partial \bar{\psi}}{\partial \bar{r}} \frac{\partial \bar{T}_f}{\partial \bar{z}} - \frac{\partial \bar{\psi}}{\partial \bar{z}} \frac{\partial \bar{T}_f}{\partial \bar{r}} \right] = \left(\frac{1}{\bar{r}} \frac{\partial}{\partial \bar{r}} \left(\left(1 + \frac{4R_d}{3} \right) \bar{r} \frac{\partial \bar{T}_f}{\partial \bar{r}} \right) + \frac{\partial^2 \bar{T}_f}{\partial \bar{z}^2} \right) + H(\bar{T}_s - \bar{T}_f) \tag{12}$$

$$\left(\frac{1}{\bar{r}} \frac{\partial}{\partial \bar{r}} \left(\left(1 + \frac{4R_d}{3} \right) \bar{r} \frac{\partial \bar{T}_s}{\partial \bar{r}} \right) + \frac{\partial^2 \bar{T}_s}{\partial \bar{z}^2} \right) = H\gamma(\bar{T}_s - \bar{T}_f) \tag{13}$$

The boundary conditions take the form as

$$\text{at } \bar{r} = r_i, \quad \bar{\psi} = 0, \quad \bar{T}_f = \bar{T}_s = \frac{1}{2} \tag{14a}$$

$$\text{at } \bar{r} = r_o, \quad \bar{\psi} = 0, \quad \bar{T}_f = \bar{T}_s = -\frac{1}{2} \tag{14b}$$

The heat transfer rate is predicted in terms of Nusselt number at hot and cold wall of the annulus using following expressions:

For fluid

$$\overline{Nu}_f = -\frac{1}{\bar{z}} \int_0^{\bar{z}} \left(\frac{\partial \bar{T}_f}{\partial \bar{r}} \right)_{\bar{r}=\bar{r}_i, \bar{r}_o} d\bar{z} \tag{15}$$

For solid

$$\overline{Nu}_s = -\frac{1}{\bar{z}} \int_0^{\bar{z}} \left(\left(1 + \frac{4}{3} R_d \right) \frac{\partial \overline{T}_s}{\partial \bar{r}} \right)_{\bar{r}=\bar{r}_1, \bar{r}_o} d\bar{z} \quad (16)$$

The total heat transfer rate from the surface is the sum of heat transferred to the fluid and solid phases as given in Ref. [15]. The total heat transfer rate for the present problem can be expressed as

$$q_t = \left\{ \phi k_f \left(\frac{\partial T_f}{\partial r} \right)_{r=r_1, r_o} + (1 - \phi) k_s \left(1 + \frac{4}{3} R_d \right) \left(\frac{\partial T_s}{\partial r} \right)_{r=r_1, r_o} \right\} \quad (17a)$$

Using Eq. (17a), it can be shown that the average total Nusselt number is

$$\overline{Nu}_t = \left(\frac{-1}{\gamma + 1} \right) \frac{1}{\bar{z}} \times \int_0^{\bar{z}} \left\{ \gamma \left(\frac{\partial \overline{T}_f}{\partial \bar{r}} \right)_{\bar{r}=\bar{r}_1, \bar{r}_o} + \left(1 + \frac{4}{3} R_d \right) \left(\frac{\partial \overline{T}_s}{\partial \bar{r}} \right)_{\bar{r}=\bar{r}_1, \bar{r}_o} \right\} d\bar{z} \quad (17b)$$

3. Numerical method

In the present study, finite element method is used to solve the coupled partial differential equations (11)–(13), subjected to boundary conditions (14). The partial differential equations are converted to matrix form of equations by using the Galerkin method. The domain is discretised into elements with the help of 3-noded triangular elements. The variation of temperature and stream function inside the element can be expressed as

$$\overline{T}_f = \overline{T}_{f1} N_1 + \overline{T}_{f2} N_2 + \overline{T}_{f3} N_3 \quad (18a)$$

$$\overline{T}_s = \overline{T}_{s1} N_1 + \overline{T}_{s2} N_2 + \overline{T}_{s3} N_3 \quad (18b)$$

$$\overline{\psi} = \overline{\psi}_1 N_1 + \overline{\psi}_2 N_2 + \overline{\psi}_3 N_3 \quad (18c)$$

where N_1 , N_2 and N_3 are the shape functions given as

$$N_i = \frac{a_i + b_i x + c_i y}{2A}, \quad i = 1, 2, 3 \quad (19)$$

In the above equation a_i , b_i , c_i are matrix coefficients.

In depth FEM formulations are discussed in the books [25,26]. The coupled matrix equations for elements are assembled in a global matrix for the whole domain, which is solved iteratively, to obtain \overline{T}_f , \overline{T}_s and $\overline{\psi}$ in the porous medium. The iterative process continues until the tolerance level of 10^{-5} , 10^{-5} and 10^{-7} for \overline{T}_f , \overline{T}_s and $\overline{\psi}$, respectively is achieved. The above mentioned tolerance level indicates the difference in the values of each of the solution variables at all nodes in the domain between two successive iterations. The domain has varying sizes of elements. Smaller sized elements are placed near the surfaces of vertical annulus due to large variations in the solution parameter near the surfaces. The smaller sized elements near the surface ensures better accuracy in calculating \overline{T}_f , \overline{T}_s and $\overline{\psi}$. The

Table 1

Comparison of results for different aspect ratio at $Ra = 100$, $Rr = 1$, $R_d = 0$

| Aspect ratio | \overline{Nu} | | | |
|--------------|-----------------|-----------|-----------|---------|
| | Ref. [7] | Ref. [10] | Ref. [27] | Present |
| 3 | 3.70 | 3.868 | 3.81 | 3.8838 |
| 5 | 3.00 | 3.025 | 3.03 | 3.0638 |
| 8 | 2.35 | 2.403 | 2.45 | 2.4249 |

Table 2

Comparison of results for different radius ratio at $R_d = 0$

| Ar | Ra | Rr | \overline{Nu} | |
|-----|------|-------|----------------------|---------|
| | | | Rajamani et al. [10] | Present |
| 5 | 50 | 0.25 | 1.619 | 1.7117 |
| | | 1 | 2.105 | 2.1800 |
| | 100 | 0.25 | 2.349 | 2.4596 |
| | | 1 | 3.025 | 3.0859 |
| 200 | 0.25 | 3.694 | 3.7034 | |
| | 1 | 4.630 | 4.5618 | |

mesh is symmetric about the vertical and horizontal central axis. Sufficiently dense mesh is chosen to make the solution mesh invariant. The present method is verified by comparing the results with previously published data [7,10,27] for the case of thermal equilibrium modeling since there is no data available in the literature pertaining to thermal non-equilibrium model for the case of vertical annulus. The data for comparison with the thermal equilibrium model is obtained by setting the variables $H = 1000$ and $\gamma = 1000$ at which the thermal equilibrium condition is recovered. Tables 1 and 2 show the comparative results. It is obvious from these tables that the present method has good accuracy in predicting the heat transfer behavior of the porous medium filled in a vertical annulus.

4. Results and discussion

The heat transfer through the porous annulus is presented in terms of the isotherms and Nusselt number for the fluid and solid phases for various values of different parameters.

Fig. 1 depicts the isotherms of fluid and solid phases inside the porous medium for different values of aspect ratio at $Ra = 100$, $R_d = 1$, $H = 5$, $\gamma = 1$ and $Rr = 1$. Aspect ratio is defined as the ratio of height of porous medium to the thickness of porous medium. The fluid isotherms move away from the vertical surface when aspect ratio is increased from 1 to 3, whereas the solid phase isotherms do not vary much with respect to the increase in aspect ratio. This is due to the reason that the heat transfer rate in solid phase is not much affected when the non-equilibrium effect is high. The influence of radius ratio on the isotherms is shown in Fig. 2 which corresponds to $Ra = 100$, $R_d = 1$, $H = 5$, $\gamma = 1$ and $Ar = 1$. The radius ratio is defined as the ratio of thickness of porous medium to the inner radius of the annulus. The isotherms of fluid as well

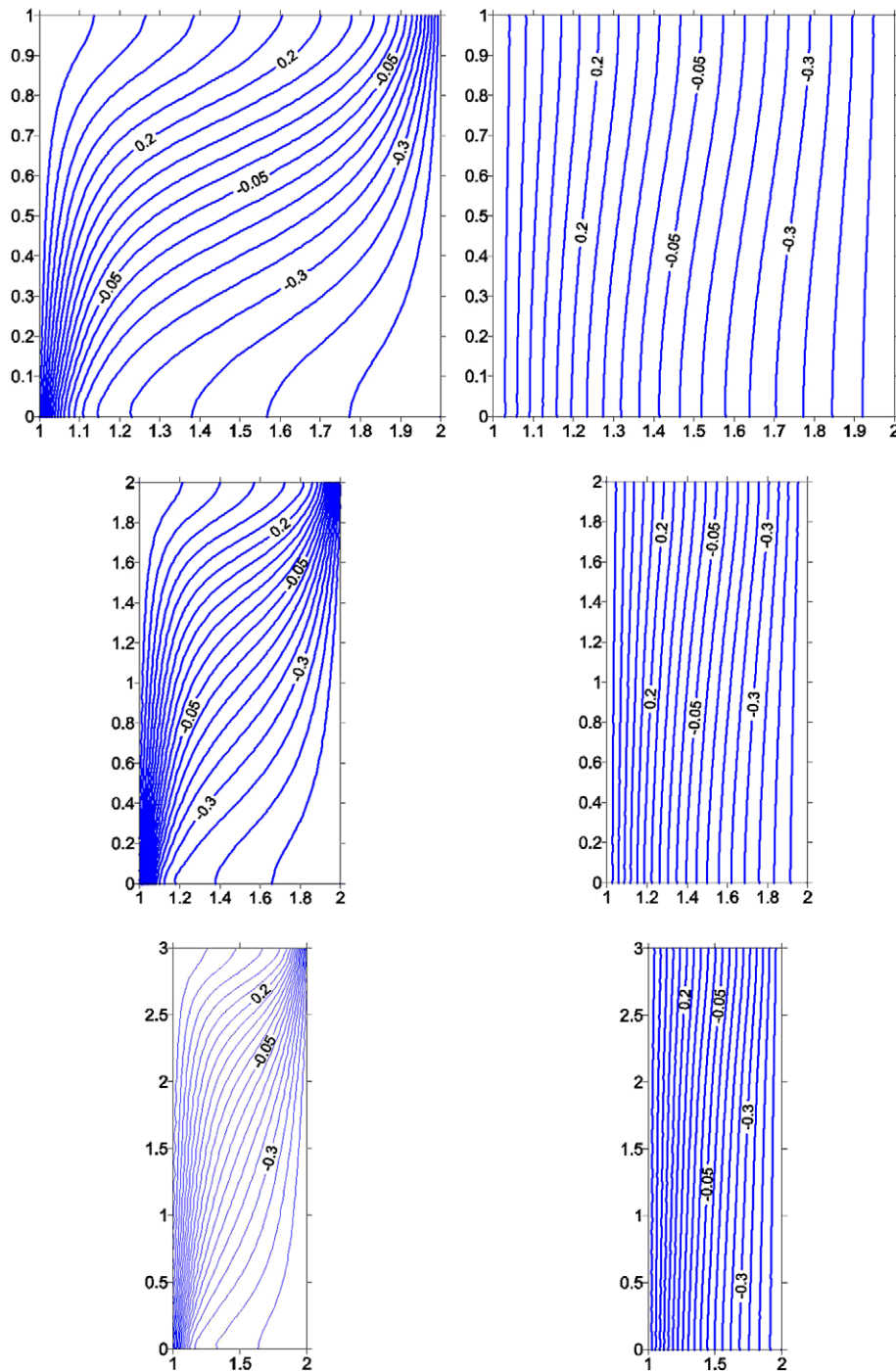


Fig. 1. Isotherms for fluid (left) and solid (right) for $Ar = 1, 2$ and 3 (Ar in increasing order from top until bottom).

as solid phases tend to move towards the hot surface and away from cold surface of the vertical annulus when the radius ratio is increased. This results in the increased thermal gradient at the hot surface and decreased thermal gradient at the cold surface. This alludes that the heat transfer rate increases at the hot surface and decreases at cold surface when radius ratio is increased. The effect of H on the isothermal lines of fluid and solid is demonstrated in Fig. 3 which is obtained at $Ra = 100$, $R_d = 1$, $R_r = 1$, $\gamma = 1$ and $Ar = 1$. The fluid isotherms are not much

affected due to change in H but the solid isotherms are affected to greater extent. At low value of H the solid isotherms are parallel to vertical surface of annulus. As H increases the solid isotherms starts deviating from being parallel to hot surface. It can be seen that the solid and fluid isotherms look alike at high value of H indicating that the thermal equilibrium state is recovered when H takes very high value. This happens due to the reason that higher value of H enhances the heat transfer between the two phases thus making the fluid and solid to attain equal

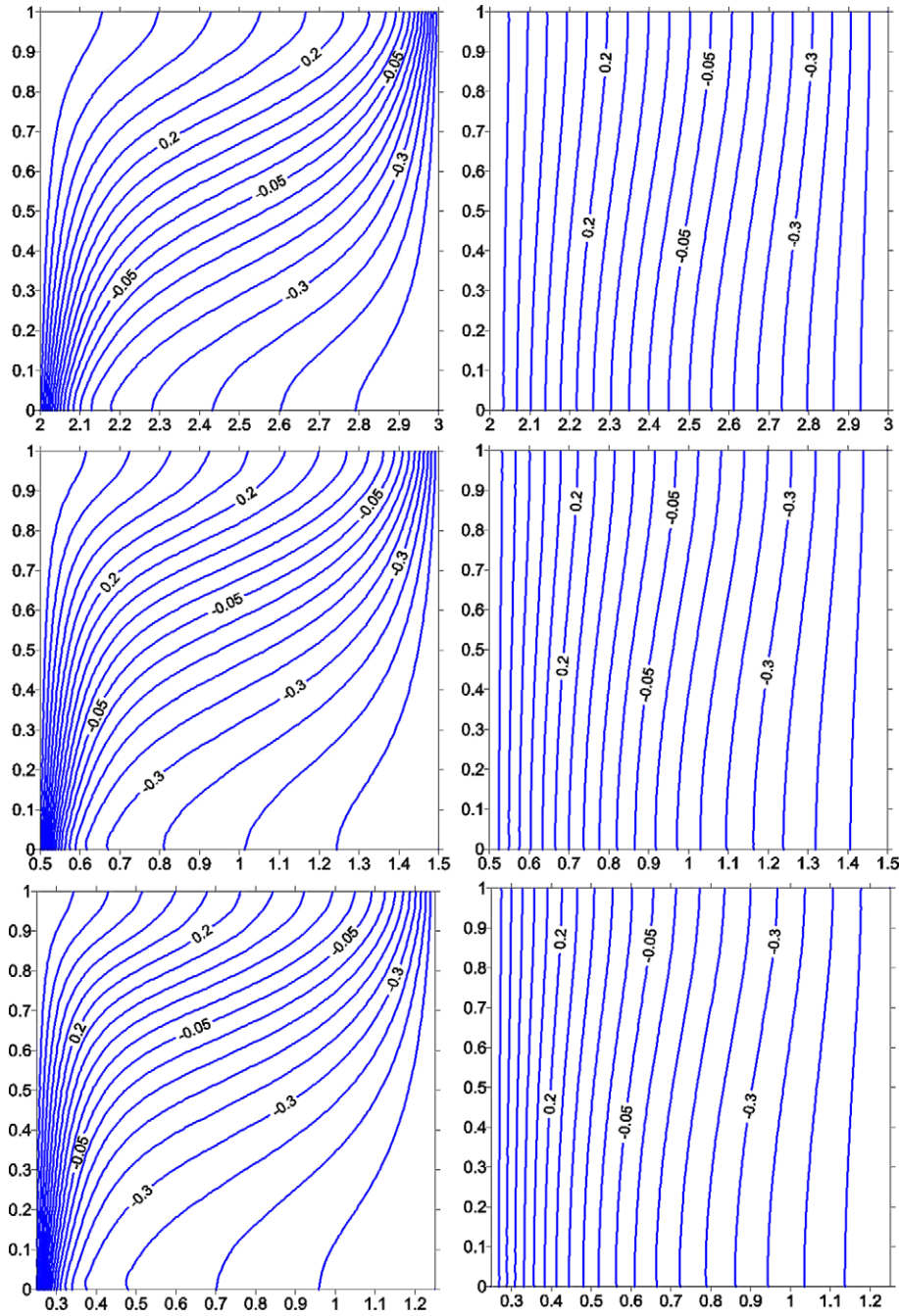


Fig. 2. Isotherms for fluid (left) and solid (right) for $Rr = 0.5, 2$ and 5 (Rr in increasing order from top until bottom).

temperature. Fig. 4 shows the isotherms for solid and fluid for various values of thermal conductivity ratio. This figure corresponds to the values $Ra = 100$, $R_d = 1$, $Rr = 1$, $H = 10$ and $Ar = 1$. The fluid isotherms move towards the bottom portion of hot and top portion of cold surface when γ is increased, thus increasing the heat transfer rate in these regions of annulus. Here also the solid isotherms are affected to greater extent as compared to the fluid isotherms. The solid isotherms are parallel to the vertical surface when γ is small. When γ is small then major part of the heat is transferred by conduction in the solid phase and partly by fluid phase. This is due to the fact that smaller

γ leads to lesser thermal resistance in the solid phase. On the contrary, the major portion of heat is transferred by the fluid phase when γ is high due to lesser thermal resistance in the fluid phase. The fluid and solid isotherms look alike at high value of thermal conductivity ratio thus leading to thermal equilibrium state.

Fig. 5 shows the effect of aspect ratio Ar , on the average Nusselt number at hot surface of the cylinder. Figs. 5 and 6 are obtained for the values $Ra = 100$, $R_d = 1$, $H = 5$ and $Rr = 1$. The Nusselt number of the fluid \overline{Nu}_f , solid \overline{Nu}_s and the total Nusselt number \overline{Nu}_t , increases with increase in thermal conductivity ratio, γ . As expected, the Nusselt

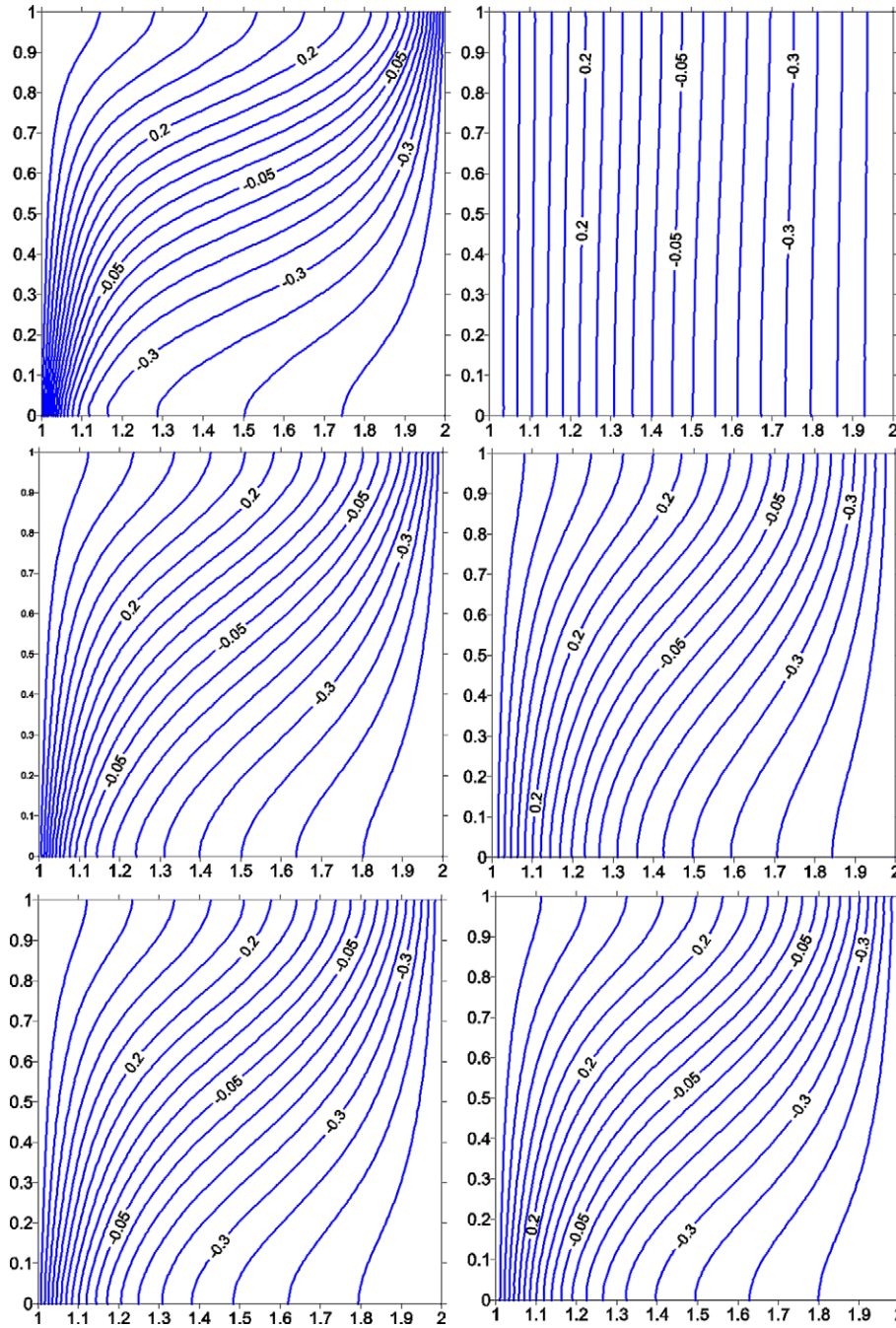


Fig. 3. Isotherms for fluid (left) and solid (right) for $H = 1, 100$ and 1000 (H in increasing order from top until bottom).

number of fluid initially increases with the increase in aspect ratio, reaches a maximum value and then starts declining. The Nusselt number of solid \overline{Nu}_s , vary negligibly with respect to aspect ratio when thermal conductivity ratio is smaller. Thus the trend of total Nusselt number \overline{Nu}_t is largely determined by the effect of \overline{Nu}_f when the value of γ is small. At higher values of γ the total Nusselt number approaches the value of \overline{Nu}_f . The influence of γ is more on \overline{Nu}_s as compared to that on \overline{Nu}_f . Similar trend of Nusselt number is observed at cold surface of annulus (figure not shown to conserve the space). However it is found that the value of Nusselt number at cold surface is lower than

corresponding value at hot surface. The difference in Nusselt number at hot and cold surfaces arises because of the fact that the domain has cylindrical geometry. Due to cylindrical nature, the inner-circumferential area is lesser than the outer-circumferential area thus the heat flowing from smaller circumferential area is distributed to larger outer-circumferential area which leads to reduction in the Nusselt number at outer surface. It is clear from Fig. 6 that the variation in aspect ratio has negligible effect on \overline{Nu}_s when $\gamma < 2$. It may be noted that the smaller values of either γ or H leads to stronger non-equilibrium effect which is also reported by authors [13,15] while studying the heat

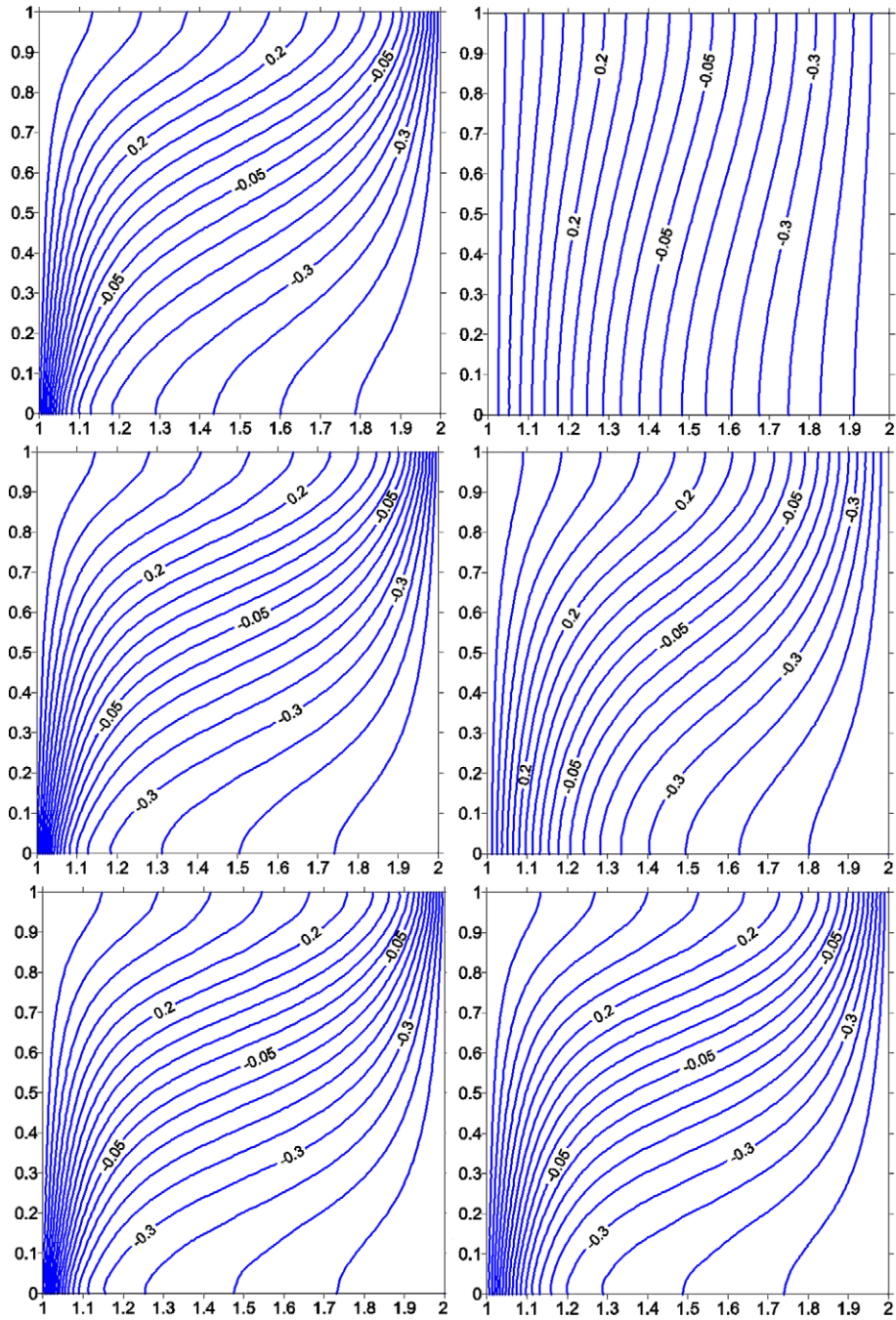


Fig. 4. Isotherms for fluid (left) and solid (right) for $\gamma = 1, 10$ and 100 (γ in increasing order from top until bottom).

transfer behavior in a square porous cavity and vertical porous layer, respectively. It is observed that when the non-equilibrium effect is stronger then variation of aspect ratio does not influence \overline{Nu}_s , although it affects the fluid Nusselt number.

Figs. 7 and 8 shows the variations of average Nusselt number at hot surface when the inter-phase heat transfer coefficient, H is varied. Figs. 7 and 8 corresponds to the values $Ra = 100$, $R_d = 1$, $\gamma = 1$ and $Rr = 1$. The \overline{Nu}_f decreases with increase in the value of H whereas the \overline{Nu}_s increases with increase in H . This happens because of the

reason that the increase in inter-phase heat transfer coefficient enhances the exchange of thermal energy from solid phase to the fluid phase due to which the temperature of the fluid increases and that of the solid decreases near the hot surface. The increase in the fluid temperature reduces the temperature difference between the hot surface and the fluid phase, which in turn decreases the temperature gradient, thus the fluid Nusselt number decreases. On the other hand when H increases, the transfer of heat from solid to fluid reduces the solid phase temperature thus increasing the temperature difference between the hot sur-

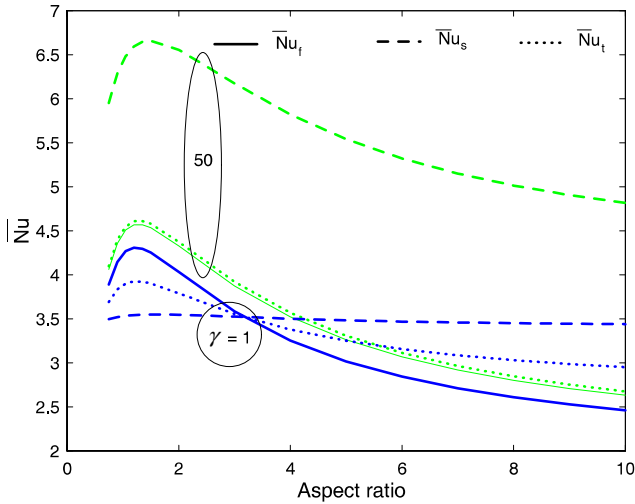


Fig. 5. \overline{Nu} variations with respect to Ar and γ at hot surface.

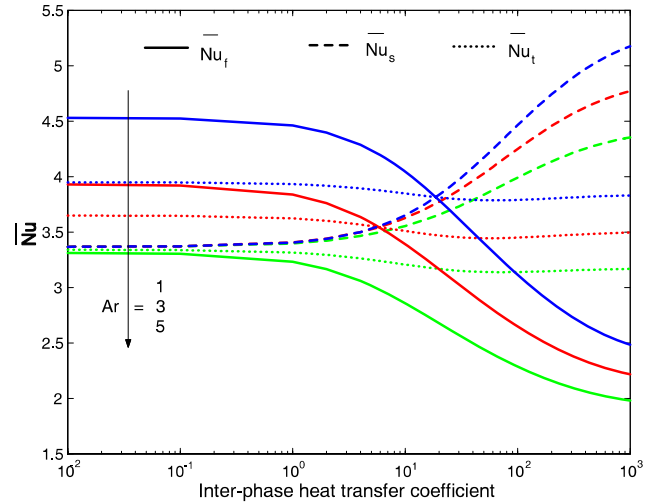


Fig. 8. \overline{Nu} vs. H at different values of Ar .

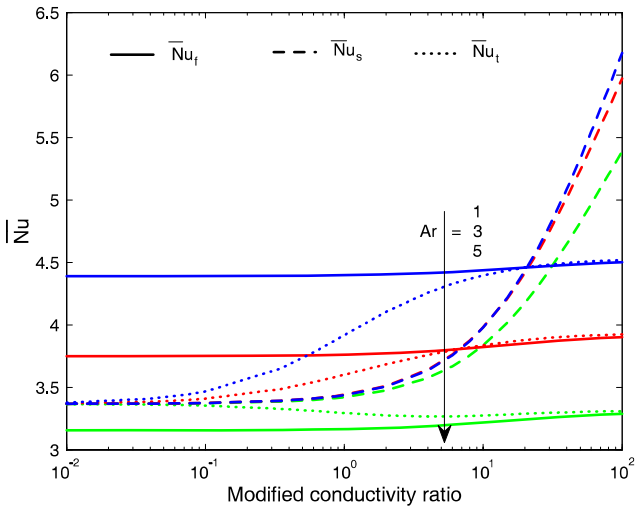


Fig. 6. \overline{Nu} vs. γ for different values of Ar .

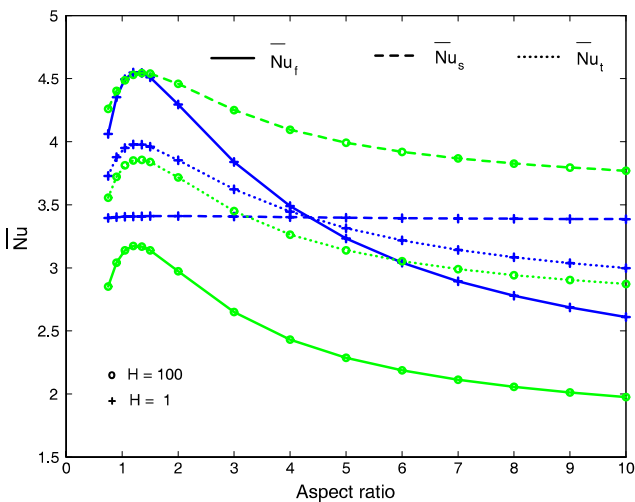


Fig. 7. \overline{Nu} variations with respect to Ar and H at hot surface.

face and solid phase. This leads to increase in the Nusselt number of solid phase. In this case also the variation of \overline{Nu}_s with respect to aspect ratio is negligible when the value of H is smaller. The decrease of the fluid Nusselt number has greater impact on total Nusselt number leading to decrease in \overline{Nu}_t even though \overline{Nu}_s increases with respect to increase in H . It is obvious from Fig. 8 that for a given aspect ratio, the variation in Nusselt number is negligible at $H < 10$. Similar trend but with lower value of Nusselt number is observed at cold surface of the annulus.

Fig. 9 illustrates the effect of radius ratio on the Nusselt number with respect to γ for the hot as well as cold surfaces of the annulus. This figure corresponds to the value $Ra = 100$, $R_d = 1$, $H = 5$ and $Ar = 2$. In general, the Nusselt number at hot surface of annulus increases with increase in radius ratio. However Nusselt number at cold surface decreases with increase in radius ratio. For a given value of Ar , H , Ra and R_d , the difference between Nusselt number at hot and cold surfaces increases with increase in

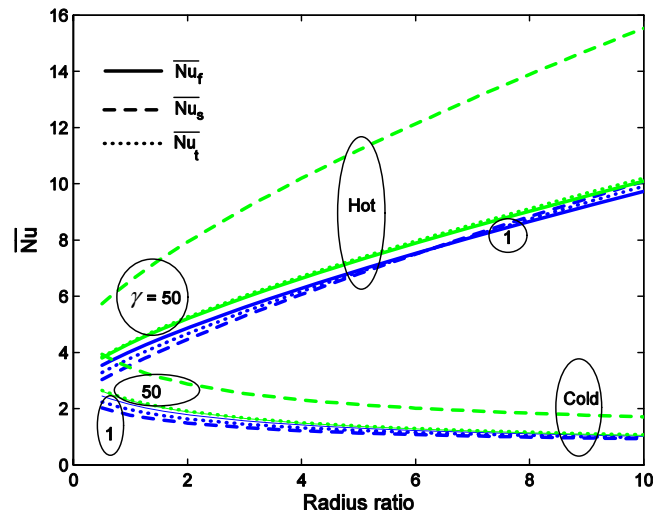


Fig. 9. \overline{Nu} variations with respect to Rr and γ .

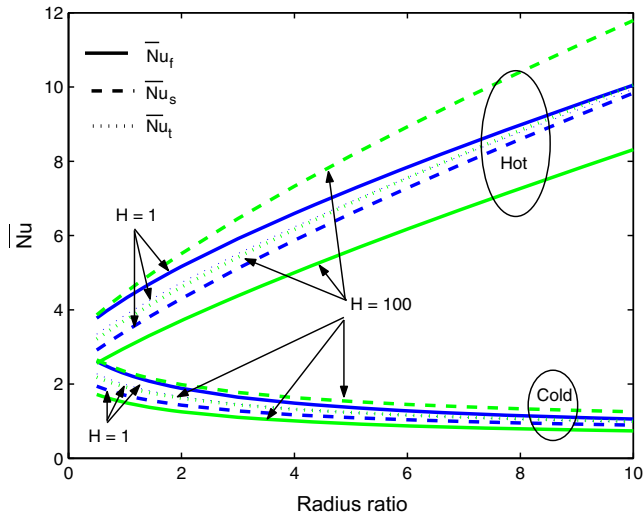


Fig. 10. \overline{Nu} variations with respect to R_r and H .

radius ratio due to enlargement of the outer-circumference of the annulus. The effect of H and radius ratio is depicted in Fig. 10 which is obtained for the values $Ra = 100$, $R_d = 1$, $\gamma = 1$ and $Ar = 2$. It is obvious from this figure that the total Nusselt number does not vary much with respect to H . \overline{Nu}_t increased by 2.13 times when radius ratio is changed from 0.5 to 10 at $H = 100$. The corresponding decrease in \overline{Nu}_t at cold surface is found to be 0.54 times when radius ratio is increased from 0.5 to 10.

Fig. 11 shows the effect of radiation parameter R_d on the average Nusselt number at hot surface for the values $Ra = 100$, $Ar = 4$, $\gamma = 2$ and $R_r = 1$. The effect of radiation parameter is more pronounced on the Nusselt number of solid as compared to that of Nusselt number of the fluid. The \overline{Nu}_s increases due to increase in radiation parameter. For a given value of radiation parameter the increase in \overline{Nu}_s is sharp for $H > 10$. The Nusselt number of fluid remains constant with respect to radiation parameter for $H < 10$ and thereafter it decreases owing to increase in radi-

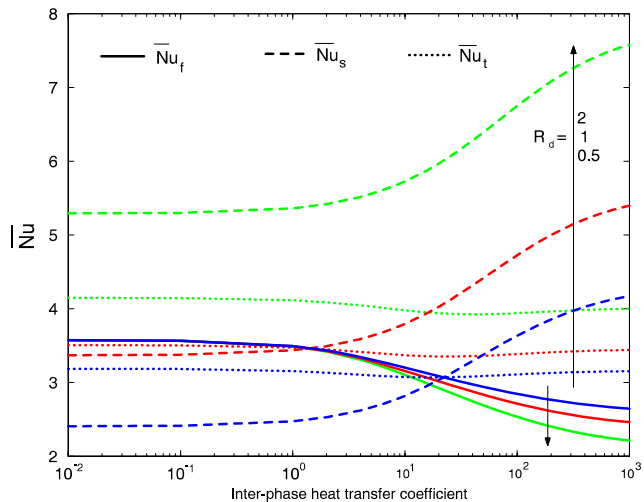


Fig. 11. Effect of H and R_d on the Nusselt number.

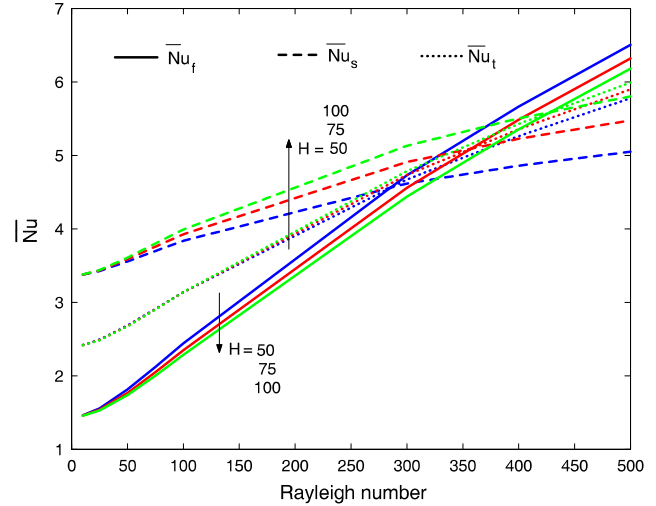


Fig. 12. Effect of Ra and H on the Nusselt number.

ation parameter. Total Nusselt number also increases with increase in radiation parameter. The contribution of \overline{Nu}_s is higher in increasing the \overline{Nu}_t as compared to that of \overline{Nu}_f . The influence of Rayleigh number on the Nusselt number is shown in Fig. 12. This figure is obtained for the values $R_d = 1$, $Ar = 5$, $\gamma = 2$ and $R_r = 1$. The Nusselt number increases with increase in Rayleigh number as expected. It is found that the \overline{Nu}_s is higher than \overline{Nu}_f at smaller values of Rayleigh number but \overline{Nu}_s is lesser than \overline{Nu}_f at higher values of Rayleigh number. This happens because; at higher Rayleigh number the buoyancy force is high which leads to faster fluid moment and thus higher heat transfer in fluid phase.

5. Conclusion

The problem of heat transfer through saturated porous medium filled in a vertical annular cylinder is investigated by using two-temperature thermal non-equilibrium model. The finite element method is utilized to solve the governing partial differential equations. The results show that the isotherms of fluid as well as solid phase move towards the hot surface and away from cold surface when radius ratio is increased. It is found that when inter-phase heat transfer coefficient and modified conductivity ratio take high value then thermal equilibrium is approached with both solid and fluid phases having similar temperature. It is found that the Nusselt number of the solid phase does not vary much with respect to aspect ratio of the annulus when the inter-phase heat transfer coefficient and the modified conductivity ratio is small. The Nusselt number of the fluid phase decreases with increase in the value of H whereas the Nusselt number of the solid increases with increase in H . It is observed that, for a given value of Ar , H , Ra and R_d the difference between Nusselt number at hot and cold surfaces increase with increase in the radius ratio. The \overline{Nu}_s increases with increase in radiation parameter. \overline{Nu}_f remains constant for $H < 10$ and thereafter decreases with increase in

radiation parameter. It is seen that the \overline{Nu}_s is higher than \overline{Nu}_f at smaller values of Rayleigh number and vice-versa at higher values of Rayleigh number.

Acknowledgement

The authors would like to thank Universiti Sains Malaysia for providing facilities under IRPA project.

References

- [1] D.A. Nield, A. Bejan, *Convection in Porous Media*, second ed., Springer-Verlag, New York, 1999.
- [2] K. Vafai, *Handbook of Porous Media*, Marcel Dekker, New York, 2000.
- [3] I. Pop, D.B. Ingham, *Convective Heat Transfer: Mathematical and Computational Modeling of Viscous Fluids and Porous Media*, Pergamon, Oxford, 2001.
- [4] D.B. Ingham, I. Pop (Eds.), *Transport Phenomena in Porous Media*, vol. II, Pergamon, Oxford, 1998.
- [5] K.A. Yih, Radiation effect on natural convection over a vertical cylinder embedded in a porous media, *Int. Comm. Heat Mass Transfer* 26 (1999) 259–267.
- [6] M.A. Hossain, M.A. Alim, Natural convection radiation interaction on boundary layer flow along a thin vertical cylinder, *Heat and Mass Transfer*, vol. 32, Springer-Verlag, 1997, pp. 515–520.
- [7] V. Prasad, F.A. Kulacki, Natural convection in a vertical porous annulus, *Int. J. Heat Mass Transfer* 27 (1984) 207–219.
- [8] V. Prasad, Numerical study of natural convection in a vertical, porous annulus with constant heat flux on the inner wall, *Int. J. Heat Mass Transfer* 29 (1986) 841–853.
- [9] V. Prasad, F.A. Kulacki, A.V. Kulkarni, Free convection in a vertical, porous annulus with constant heat flux on the inner wall—experimental results, *Int. J. Heat Mass Transfer* 29 (1986) 713–723.
- [10] R.C. Rajamani, C. Srinivas, P. Nithiarasu, K.N. Seetharamu, Convective heat transfer in axisymmetric porous bodies, *Int. J. Numer. Methods Heat Fluid Flow* 5 (1995) 829–837.
- [11] D.A.S. Rees, A.P. Bassom, I. Pop, Forced convection past a heated cylinder in a porous medium using a thermal non-equilibrium model: boundary layer analysis, *Eur. J. Mech. B/Fluids* 22 (2003) 473–486.
- [12] S.W. Wong, D.A.S. Rees, I. Pop, Forced convection past a heated cylinder in a porous medium using a thermal non-equilibrium model: finite Peclet number effects, *Int. J. Thermal Sci.* 43 (2004) 213–220.
- [13] A.C. Baytas, I. Pop, Free convection in a square porous cavity using a thermal non-equilibrium model, *Int. J. Thermal Sci.* 41 (2002) 861–870.
- [14] Pei-Xue Jiang, Ze-Pei Ren, Numerical investigation of forced convection heat transfer in porous media using a thermal non-equilibrium model, *Int. J. Heat Fluid Flow* 22 (2001) 102–110.
- [15] N.H. Saeid, Analysis of mixed convection in a vertical porous layer using non-equilibrium model, *Int. J. Heat Mass Transfer* 47 (2004) 5619–5627.
- [16] N.H. Saeid, A.A. Mohamad, Periodic free convection from a vertical plate in a saturated porous medium non-equilibrium model, *Int. J. Heat Mass Transfer* 48 (2005) 3855–3863.
- [17] A. Marafie, K. Vafai, Analysis of non-Darcian effects on temperature differentials in porous media, *Int. J. Heat Mass Transfer* 44 (2001) 4401–4411.
- [18] B. Cherif, M.S. Sifaoui, Numerical study of heat transfer in an optically thick semi-transparent spherical porous medium, *J. Quant. Spectrosc. Radiat. Transfer* 91 (2005) 363–372.
- [19] B. Cherif, M.S. Sifaoui, Theoretical study of heat transfer by radiation conduction and convection in a semi-transparent porous medium in a cylindrical enclosure, *J. Quant. Spectrosc. Radiat. Transfer* 83 (2004) 519–527.
- [20] T. Sghaier, B. Cherif, M.S. Sifaoui, Theoretical study of combined radiative conductive and convective heat transfer in a semi-transparent porous medium in a spherical enclosure, *J. Quant. Spectrosc. Radiat. Transfer* 75 (2002) 257–271.
- [21] D.A.S. Rees, I. Pop, Free convective stagnation point flow in a porous medium using thermal non-equilibrium model, *Int. Comm. Heat Mass Transfer* 26 (1999) 945–954.
- [22] D.A.S. Rees, I. Pop, Free convection boundary-layer flow in a porous medium using thermal non-equilibrium model, *J. Porous Media* 3 (2000) 31–43.
- [23] M.F. Modest, *Radiative Heat Transfer*, McGraw-Hill, New York, 1993.
- [24] A. Raptis, Radiation and free convection flow through a porous medium, *Int. Comm. Heat Mass Transfer* 25 (1998) 289–295.
- [25] L.J. Segerland, *Applied Finite Element Analysis*, John Wiley and Sons, New York, 1982.
- [26] R.W. Lewis, P. Nithiarasu, K.N. Seetharamu, *Fundamentals of the Finite Element Method for Heat and Fluid Flow*, John Wiley and Sons, Chichester, 2004.
- [27] S.K. Nath, V.V. Satyamurthy, Effect of aspect ratio and radius ratio on free convection heat transfer in a cylindrical annulus filled with porous media, HMT C16-85, in: *Proc. 8th Nat. Heat and Mass Transfer Conf.*, India, 1985, pp. 189–193.